Journal of ELECTRONIC MATERIALS, Vol. 45, No. 8, 2016
DOI: 10.1007/s11664-016-4567-5

Thermal Behavior of a Medium-Frequency Ferrite-Core Power Transformer

SELAMI BALCI,[1,3] IBRAHIM SEFA,[2,4] and NECMI ALTIN[2,5]

1.—Graduate School of Natural and Applied Sciences, Gazi University, Ankara, Turkey. 2.—Department of Electrical and Electronics Engineering, Faculty of Technology, Gazi University, Besevler, 06500 Ankara, Turkey. 3.—e-mail: selamibalci@gazi.edu.tr. 4.—e-mail: isefa@gazi.edu.tr. 5.—e-mail: naltin@gazi.edu.tr

In this study, design and thermal analysis of a medium-frequency transformer with ferrite N87 core have been carried out using finite-element analysis software. A thermal model of the medium-frequency transformer is generated and analyzed with different cooling methods. In addition, it is proposed to attach additional heat sinks at the top and bottom of the transformer core. Effects of these additional heat sinks on cooling performance and sizing of the transformer are investigated. Furthermore, the cooling capacity of the proposed material is investigated, depending on the air flow velocity for the forced-air cooling method. Thus, more realistic behavior of the ferrite N87 material is obtained for a medium-frequency transformer with 35 kVA rated power and 10 kHz operating frequency. Moreover, electromagnetic and thermal analyses are carried out through linked simulations. The heat distribution in the core including saturation effect is also investigated in detail.

Key words: Medium-frequency transformer, thermal analysis, FEA, forced-air cooling, thermal behavior

INTRODUCTION

Core and winding losses create a temperature rise inside transformers. This temperature rise is a limiting factor when obtaining a desired power value in the transformer sizing process. Therefore, the thermal behavior of the determined core material plays an active role in the sizing process. The core losses of the core materials increase with the operating frequency, and in particular reach their highest values under nonsinusoidal excitation. On the other hand, the current-carrying capacities of the primary and secondary winding conductors are important parameters that affect the temperature of high-power transformers. Since skin and proximity effects vary with operating frequency, increasing the frequency value increases the alternating-current (AC) resistance of the windings and thus causes greater winding losses. This leads to additional temperature rise, which means more losses.

(Received December 18, 2015; accepted April 22, 2016; published online May 5, 2016)

Transformer losses can be significantly reduced by using soft-magnetic materials which have lower specific core losses, e.g., ferrite, amorphous, and nanocrystalline materials, for operation at higher frequency values.[1,2] The type of conductor used in windings also defines the conduction losses in medium/high-frequency transformers. In medium-frequency (MF) transformers, Litz or foil conductors are usually preferred, and their cross-sectional area is determined according to the maximum current density. However, the cooling method and utilization factor of the winding region must be considered during the core sizing step in the design process.[3]

Since rise in transformer temperature causes deterioration in magnetic and electrical parameters of the transformer, the temperature value of the transformer is another limiting parameter in core sizing of high-power MF transformers. Therefore, estimation of core and winding losses and the temperature rise is of great importance at the early design stage.[4–7] Furthermore, designers should investigate the required cooling system and its components.

The core volume can be significantly reduced by increasing the operating frequency of MF transformers. This reduction in core size also causes a reduction of the cooling surface. This may lead to a requirement for additional heat sinks to increase the cooling surface and limit the temperature rise. Sample designs for a 1-MW, 20-kHz power transformer showed that the cooling performance can be improved by attaching aluminum heat sinks to the transformer core.[8] In addition, forced-air convection and fluid cooling systems are used for cooling the windings and cores of MF transformers to obtain a more compact design.[9,10] Design parameters such as core material type, saturation flux value, operation frequency, core volume, and material thickness affect core losses. In addition, nonsinusoidal excitation conditions such as rectangular waves and pulses with modulated excitation, or harmonic components, also increase core losses and lead to an increase in core temperature. Power electronic circuits for use in electric vehicles, uninterruptible power supplies, and renewable energy sources are operated with this kind of excitation waveform at medium to high frequency.[11,12] In addition, solid-state transformers which are excited with rectangular waveforms have recently become a popular research subject for low- as well as medium-voltage applications.[13] In particular, the thermal behavior of medium/high-frequency transformers is nonlinear, depending on the nonsinusoidal excitation voltage waveform.[14–16]

In previous literature, there are many studies on thermal analysis of transformers. However, most of these studies focus on thermal testing of fluid-cooled or dry-type line frequency transformers using finite-element analysis (FEA) software, whereas studies on testing the cooling performance of medium/high-frequency transformers at the design stage are scarce. A two-dimensional (2D) electromagnetic and thermal model of a dry-type high-voltage transformer has been proposed to validate the design.[17] In addition, a three-dimensional (3D) electromagnetic model for three-phase power transformers is proposed. Loss values of the transformer are determined by electromagnetic analysis, and the temperature of the transformer is calculated for steady-state condition. However, in this study, natural convection was investigated while the effect of air flow velocity was not examined.[18] The cooling performance of high-power oil-filled line frequency transformers depending on the oil flow velocity has been investigated using coupled analysis, showing that this method increases the heat transfer capability.[19–21] The cooling performance depending on the fan speed was investigated for dry-type line frequency distribution transformers using FEA, obtaining useful data on the temperature condition of the transformer before prototyping the product.[22] Besides, the thermal behavior of the transformer has greater importance in medium/high-frequency operation conditions. In addition, determination of the performance of an air–fluid cooling system before prototyping contributes to the production process. A thermal model for a transformer with an amorphous core operating at 2 kHz has been presented, and the temperature of the transformer obtained numerically for no- and full-load conditions.[5] By using computational fluid dynamics software, the thermal effects of the transformer can be seen before prototyping. In this way, the performance of transformer cooling systems can be tested using FEA.

In this study, the design of an MF transformer with ferrite N87 core material is proposed. The losses of the designed transformer were calculated using Maxwell 3D software and the steady-state thermal behavior of the designed MF transformer analyzed. Electromagnetic and thermal analyses are carried out together for the MF transformer with a certain power capacity at medium frequency. Furthermore, the thermal behavior of the designed transformer is determined, and the performance of the forced-air cooling method tested and reported. In addition, aluminum heat sinks are attached onto the transformer core to improve the cooling performance. Afterwards, the different cooling methods are compared with one another.

THERMAL MODELING OF THE TRANSFORMER

A proper transformer thermal model should contain all heat sources inside the transformer. There are two main heat sources, namely winding and core losses, in transformers. Both core and winding losses increase with frequency, thus the dependence of temperature on operating frequency is an important factor for consideration in the MF transformer design process.

Core and Winding Losses

Various mathematical models have been proposed in literature to show the frequency effects on core losses in MF transformers used in power converters. The most useful formulation is called the Steinmetz equation, defined based on the transformer volume (V_c) as shown in Eq. 1.[5,6]

$$P_v = K f^{\alpha} B_m^{\beta}, \tag{1}$$

where K, α, and β are determined by the core material characteristics, f is the frequency of the waveform, and B_m is the magnitude of the magnetic induction in the bidirectional magnetization case.[5]

Due to the increase of power electronics-based systems in recent years, the Steinmetz equation has been revised for nonsinusoidal excitation.[23] The losses that occur in the magnetic core, depending on the variation frequency of the magnetic induction, are taken into account in this expression. The Steinmetz equation for nonsinusoidal waveforms is given in Eq. 2 per unit volume (P_v) according to the

rate of change of magnetic induction. In this equation, the modified Steinmetz coefficient (k_i) varies depending on the core material characteristics as shown in Eq. 3.[5]

$$P_v = \frac{1}{T}\int_0^T k_i \left|\frac{dB(t)}{dt}\right|^{\alpha} (\Delta B)^{\beta-\alpha} dt, \tag{2}$$

$$k_i = \frac{K}{(2\pi)^{\alpha-1}\int_0^{2\pi} |\cos\theta|^{\alpha} 2^{\beta-\alpha} d\theta}. \tag{3}$$

Then, the core losses according to the core volume (V_c) are obtained as given in Eq. 4:

$$P_{core} = P_v V_c. \tag{4}$$

The magnetic induction waveform is another important parameter that affects the core losses. The transformer core losses are given as in Eq. 5 for rectangular wave excitation:[24]

$$P_v = 2^{\alpha+\beta} k_i K f^{\alpha} B_m^{\beta}. \tag{5}$$

The heat sources used in the thermal model for the transformer are given in Eqs. 6 and 7 for the volume of the interior core (V_{cc}) and exterior core (V_{ce}), respectively.[4,5] This condition is only valid when the internal and external temperatures are different.

$$P_{cc} = P_v V_{cc}, \tag{6}$$

$$P_{ce} = P_v V_{ce}. \tag{7}$$

Single-strand round wire such as American wire gauge (AWG) is used for conductors in line frequency transformer windings. In MF transformers, the AC resistance of the conductor is affected by the skin and proximity effects. Therefore, multiple-stranded Litz wire or foil conductors are preferred for medium- to high-frequency applications to decrease the impacts of these effects. Dowell's equation given in Eq. 8 expresses the AC resistance of the conductor foil[4,25]:

$$RF = \frac{R_{ac}}{R_{dc}}, \tag{8}$$

where RF is the resistance factor. Current harmonics also affect the winding losses, and Eq. 9 can be written for the transformer winding losses by considering these current harmonic components.[4]

$$P_w = \sum_{v=1}^{n} {}^{v}R_{ac-p}^{v} I_p^2 + \sum_{v=1}^{n} {}^{v}R_{ac-s}^{v} I_s^2. \tag{9}$$

Here, all the windings in the transformer are defined as a separate heat source. The heat sources (P_p and P_s) used in the thermal model for the primary and secondary windings are given by Eqs. 10 and 11, respectively.[4]

$$P_p = \frac{N_p \rho l_p}{A_{pr}} RF \cdot I_p^2, \tag{10}$$

$$P_s = \frac{N_s \rho l_s}{A_{sc}} RF \cdot I_s^2, \tag{11}$$

where A_{pr} and A_{sc} are the cross-sectional area of the conductors of the primary and secondary windings, respectively. ρ is the conductivity, which varies with the type of conductor material. l_p and l_s are the mean length of the turns of the primary and secondary windings. Also, N_p and N_s are the number of turns of the primary and secondary windings.

Effects of Operating Frequency on Transformer Sizing and Thermal Properties

The effects of the operating frequency on the electrical and magnetic parameters of the transformer are usually considered. However, the frequency also affects the mechanical parameters of the transformer directly. Therefore, the operating frequency can be considered as the most important parameter, having a significant effect on transformer sizing and thermal properties. The relation between the operating frequency and the volume of the transformer core is given in Eq. 12[26]:

$$V_c \propto \frac{1}{\sqrt[4]{f^3}}. \tag{12}$$

Furthermore, the average temperature change of the transformer core can be determined in proportion to the frequency, as given in Eq. 13 for ferrite N87 core material.[26]

$$\Delta T \propto f. \tag{13}$$

It is seen that the temperature of the transformer with ferrite N87 core is approximately directly proportional to the operating frequency, so the amount of decrease in volume depending on the operating frequency is limited by the required cooling surface for a certain temperature.

Thermal Equivalent Circuit of the Transformer

The thermal equivalent circuit of the MF transformer with ferrite N87 core material whose thermal effects are analyzed is shown in Fig. 1.[4] The primary and secondary windings of the designed transformer are divided and placed on each of the legs. Nodes between the windings and the core are identified when creating the thermal equivalent circuit.

In the equivalent circuit, T_a is the ambient temperature, while T_{cc} and T_{ce} are the core temperatures. P_{cc} is the heat generated in the interior of the core. P_{ce} is the heat generated on the surface of the core. Also, T_p and T_s indicate the temperatures

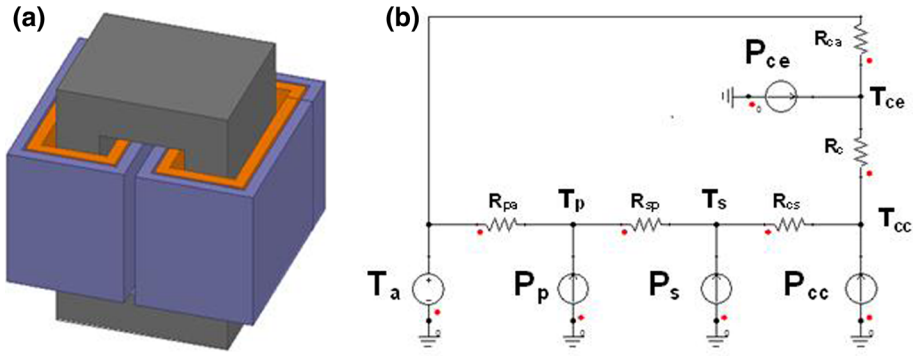

Fig. 1. 3D geometry of transformer and its simple thermal equivalent circuit.

of the transformer windings. P_p and P_s are the heat generated in the primary and secondary windings, respectively. The equivalent thermal resistance between the fluid and the solid surface (A) is a combination of the convective and radiative heat transfer resistances.[5] The equivalent thermal conductivity between a solid and a fluid is described by Eq. 14.[5,27]

$$R_{\text{th-eq}} = \frac{A}{\frac{1}{h_{cc}} + \frac{1}{h_r}}. \tag{14}$$

The heat transfer on the horizontal and vertical surfaces through both convection (h_{cc}) and radiation (h_r) according to the maximum power distribution capacity is given in Eq. 15.[4]

$$\max P_d = \max(P_{\text{conv}} + P_{\text{rad}}). \tag{15}$$

Thus, the maximum power distribution (P_d) is proportional to the minimum thermal resistance, which is a combination of the parallel convective and radiative thermal resistances, as expressed in Eq. 16.[4]

$$\min R_{sa} = \min\left(\frac{R_{\text{conv}} R_{\text{rad}}}{R_{\text{conv}} + R_{\text{rad}}}\right) = \min\left(\frac{1}{h_{cc}A + h_r A}\right). \tag{16}$$

The heat dissipation capacity according to the relationship between the convective and radiative coefficients is also given in Eq. 17.[4]

$$\max P_d \propto \max(h_{cc}A + h_r A). \tag{17}$$

Convective and radiative boundary conditions can be used for fluid-cooled systems. Because the radiation in Eq. 18 is negligibly small, the released heat is mostly transferred to the fluid by forced convection[28,29]:

$$P_d = h \cdot A \cdot (T - T_a). \tag{18}$$

The convective heat transfer coefficient on the outer surface of the forced-air-cooled transformer varies depending on the air flow velocity. Therefore, the convective coefficient can be expressed approximately using Eq. 19, when the air flow velocity varies between 0 m/s and 25 m/s[30]:

$$h = h_0 + 4.0 \times v, \tag{19}$$

where v is the air flow velocity, and h_0 is the air convective coefficient at room temperature, whose value is accepted as 5.8 W/m^2°C approximately.[30] If air flow will not be used, h_0 may be considered as the capability for natural cooling.

Thermal 3D Modeling with Finite-Element Analysis

There are two principal methods for heat dissipation calculations: analytical methods including lumped-parameter thermal networks, and numerical techniques involving FEA for heat conduction and computational fluid dynamics.

The three-dimensional (3D) equivalent thermal network of the 3D modeled transformer is depicted in Fig. 2.[31] A separate thermal circuit representing each axis in the coordinate system is created in this network. Thereby, the thermal capacity and heat source are connected to the common node for the element.[31] In this equivalent circuit, C represents the equivalent heat capacity and q is the heat flux.

Mathematical methods are used in the transformer design process to determine the temperature increase under real operating conditions. However, the system becomes nonlinear under nonsinusoidal excitation conditions, and the solution becomes quite complex when using conventional mathematical approaches. Thus, it is much more useful to apply FEA, which allows calculations for problems by dividing them into finite elements.

All axes of the coordinate system can be separately analyzed easily by reducing the prism in this model to a one-dimensional problem. The average temperature ΔT and total heat generation in the equivalent thermal model of the x-coordinate for the prism are given in Eqs. 20 and 21, respectively[31]:

$$\Delta T = \frac{1}{l_x} \int_{-l_x/2}^{l_x/2} \frac{\dot{q} l_x^2}{2\lambda_x}\left(\frac{1}{4} - \frac{x^2}{l_x^2}\right) dx, \tag{20}$$

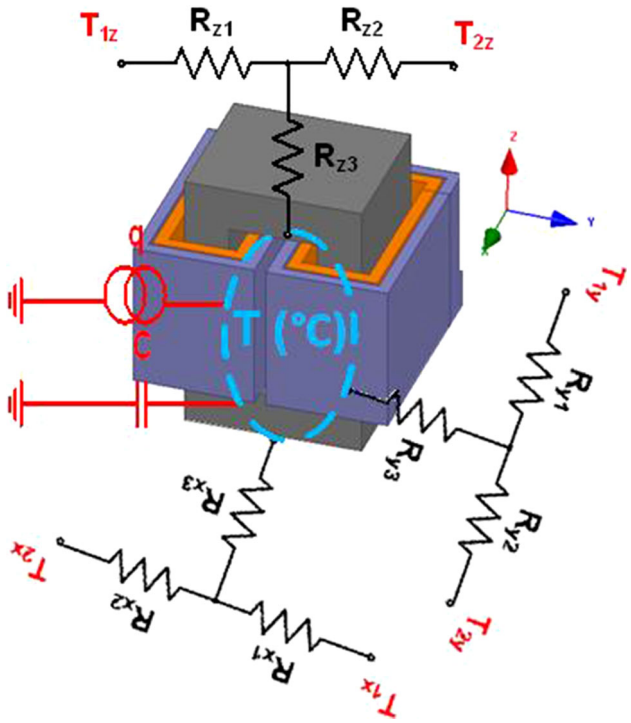

Fig. 2. 3D thermal equivalent circuit of the transformer.

$$q_x = \dot{q}V = \dot{q}A_x l_x. \tag{21}$$

Thus, Eq. 22 is used to calculate the thermal conductivity (λ) for the x plane:

$$\lambda_x = \frac{q_x l_x}{A_x \Delta T}. \tag{22}$$

A 3D thermal conductivity can be formed from this equivalent circuit as indicated in Eq. 23[31]:

$$\lambda = \begin{bmatrix} \lambda_x & 0 & 0 \\ 0 & \lambda_y & 0 \\ 0 & 0 & \lambda_z \end{bmatrix}. \tag{23}$$

DETERMINATION OF COOLING SYSTEM FOR MF TRANSFORMER

Since higher transformer temperature has negative effects on its operating parameters, the determination and design of an optimum cooling system are of great importance for transformer performance. Convection (forced-air or fluid) is used to cool the transformer core and windings. Analysis and modeling based on numerical techniques developed in recent years allow design of fluid-cooled electric machines. Fluid cooling systems are usually preferred for high-power transformers because of the closed-loop circulation requirement for fluid material, high cost, and complicated structure of these cooling systems.

Cooling methods given in Table I may be used for cooling a transformer. In this table, the fluid cooling system for high-power MF transformers offers superior performance in terms of heat absorption capacity and heat transfer capacity. Current density values of 2 A/mm^2 for natural cooling, 4 A/mm^2 for forced-air cooling, and 6 A/mm^2 to 7 A/mm^2 for fluid-cooled transformers are recommended in case of aluminum conductors.[4,26,29]

Table I. Cooling methods and heat transfer coefficients[25,28]

Cooling method	Convection coefficient (W/m^2 K)
Natural	6
Forced air	20
Forced air cooling with heat sink	200
Fluid	1800

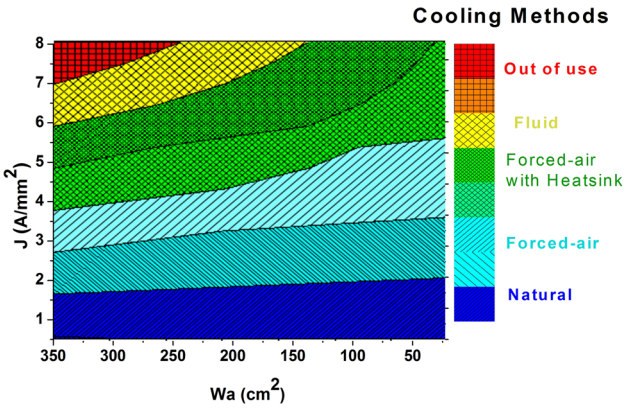

Fig. 3. Cooling requirement according to current density parameter.

The current density parameter (J) must be considered in terms of the transformer winding region (W_a) and losses when determining the thickness of the winding conductor. The colored graphics in Fig. 3 are very useful for determination of the cooling system according to the current density and winding region. While higher current density values decrease the winding volume, they increase the cooling requirement. Therefore, fluid convection is commonly used in high-power transformers to remove heat from the windings and core. In the graph, red region corresponds to values of current density larger than 7 A/mm^2, not being used in practice.

Thermal Analysis Process with FEA

In this study, thermal analysis was performed using ANSYS Fluent software. The flowchart of the performed thermal analysis is presented in Fig. 4. Transformer losses are determined in the first step of the thermal analysis. Here, the core and winding losses are calculated by FEA. Since the excitation type affects the core losses, it is also considered. In

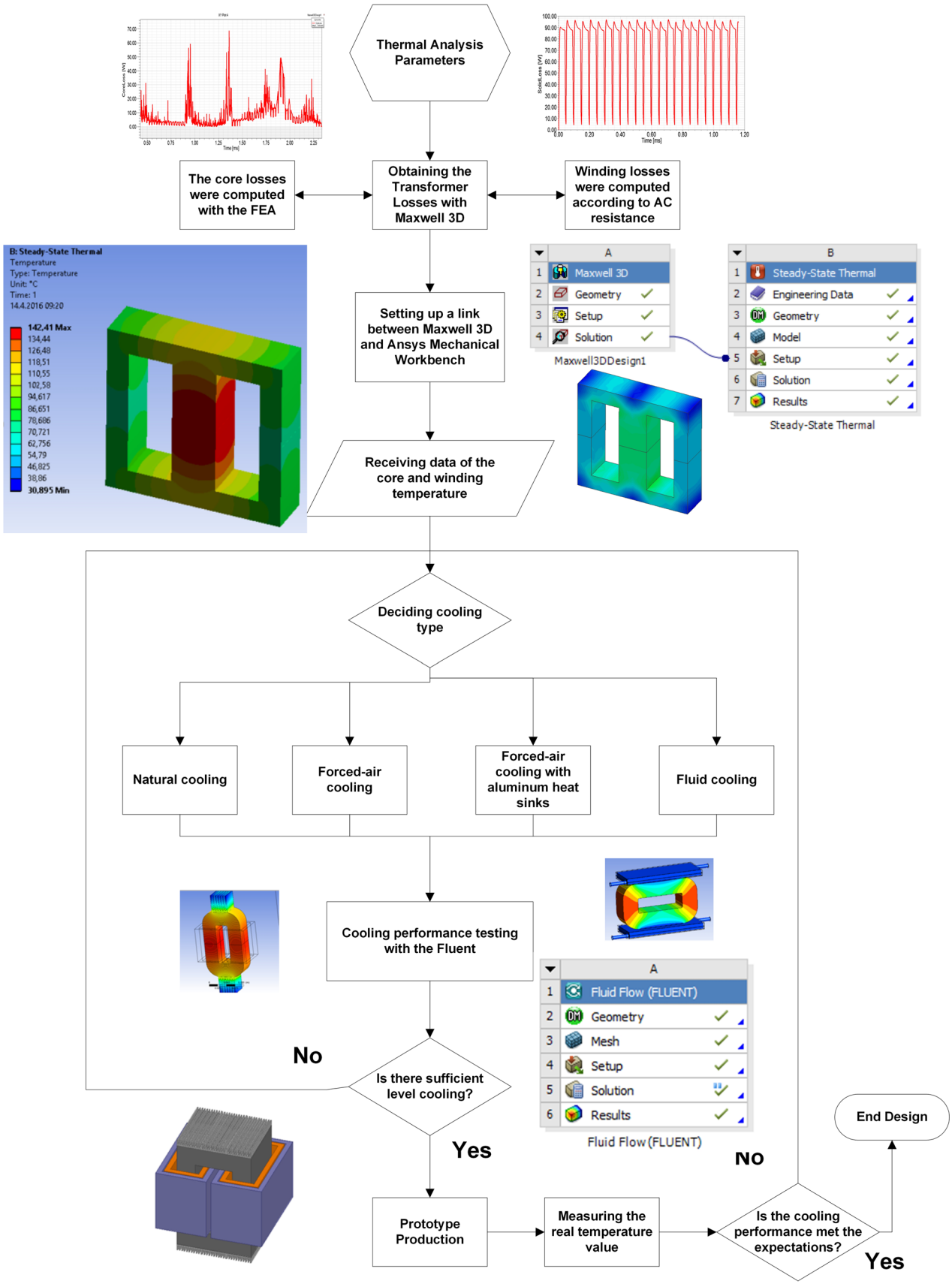

Fig. 4. Flowchart of thermal analysis process.

addition, frequency-dependent effects such as the proximity and skin effects are taken into account during the winding loss calculations. Modeling and simulation studies can be performed for almost real operating conditions by using the transient solver of the Maxwell 3D software. Simplorer and Maxwell software are operated simultaneously for performance testing of the transformer when excited by electronic circuits such as a power converter and inverter.

In the second step, loss data obtained from the Maxwell software for steady-state temperatures are linked to ANSYS Mechanical Workbench. At this stage, transient and steady-state thermal effects are computed by dividing the problem region into finite elements, and the heat dissipation can be visualized according to the maximum temperature value. Thus, temperatures in the core and windings are obtained before producing the transformer prototype. Then, the cooling method is decided in order to remove the heat generated in the core and windings. In this stage, criteria such as the ambient temperature of the transformer, the application area, the occupied space, and the weight should also be considered.

The next step is to test how much cooling can be achieved using the decided cooling method based on the fluid dynamic software before production of the prototype. For this purpose, the transformer geometry is defined in 3D in the ANSYS Fluent software. Data for the losses occurring in the core and windings are obtained from Maxwell 3D. Thus, the cooling performance can be tested with air or liquid flow. If the selected cooling system performance and capabilities are insufficient, the selected method needs to be revised. The design process is completed when the cooling performance is validated by FEA, and the transformer prototypes may be produced.

THERMAL PERFORMANCE ANALYSIS OF MF TRANSFORMER BY FEA

The full-bridge inverter circuit used to supply the transformer at 10 kHz operating frequency for the thermal analysis is shown in Fig. 5. In this circuit, the MF transformer is modeled using ANSYS–Maxwell 3D software. Then, the transformer equivalent circuit in Maxwell 3D is linked to Simplorer software, where the power electronic converter is modeled for cosimulation.[32] Simplorer and Maxwell software were cosimulated simultaneously for 1 μs time step and 10 kHz operating frequency. According to Maxwell 3D analysis reports, the flux distribution of the core is depicted for maximum 0.3 T flux values.

The data required to perform the thermal analysis of the core and winding losses of the transformer are obtained from the electromagnetic analysis (see Table II). The core and winding heat sources given in this table are required input data for the thermal analysis. These heat sources are determined in accordance with the core and winding losses computed using the FEA software.

Thermal Performance of Forced-Air Cooling Method

While there is no air flow in a vacuum environment, the radiative thermal effects at the

Table II. Thermal and electrical parameters of MF transformer

Excitation waveform	Rectangular
DC link voltage	400 V
Turn ratio	1:1
Rated power	35 kVA
Rated current	78.7 A_{rms}
Switching frequency	10 kHz
Core material	Ferrite N87
Thermal conductivity (λ)	0.004 W/m-K
Convection coefficient (h_c)	10 W/m^2°C
Winding material	Aluminum foil (100×0.4 mm^2)
Saturation flux density	0.39 T
Max. flux density (for 10 kHz)	0.20 T
Core volume	1614 cm^3
Core losses	128 W
Core heat source	79,306 W/m^3
Winding volume	750 cm^3
Winding losses	150 W
Winding heat source	200,000 W/m^3

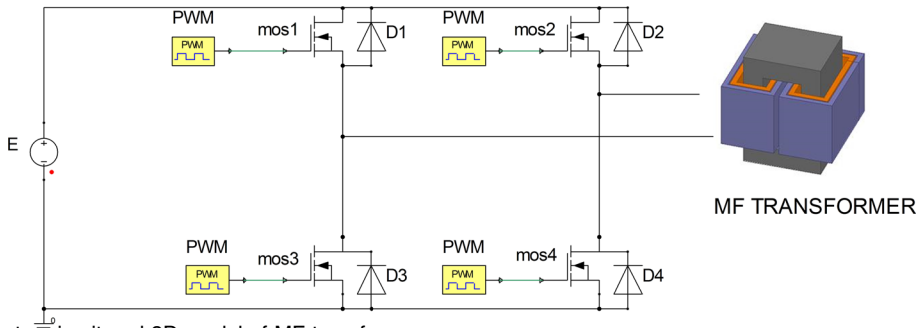

Fig. 5. Full-bridge inverter circuit and 3D model of MF transformer.

transformer surfaces are shown in Fig. 6a. Here, the temperature distribution is given for the maximum 400 K. It is also seen that the primary winding heats more than the secondary winding, and this leads to an additional rise in core temperature. This effect may be removed by a gap between the primary and secondary windings and between the windings and the core.

In case of natural convection with 0.5 m/s air velocity, the temperature distribution on the transformer is given in Fig. 6b for maximum 331 K. Here, the cooling is obtained through natural convection, and the transformer temperature is kept at approximately 69°C. This shows the effect of natural air circulation in unhoused dry-type transformers clearly.

The temperature distribution with 1 m/s air velocity is given in Fig. 6c for maximum 326 K. The variation of the cooling capability with the air flow velocity in the forced-air cooling method can be clearly seen from this figure. The cooling air circulation is passed through the air gap between the windings and core of the transformer along the *z*-plane and transfers the heat. Thus, the temperature difference is about 5°C between the upper and lower parts of the transformer core.

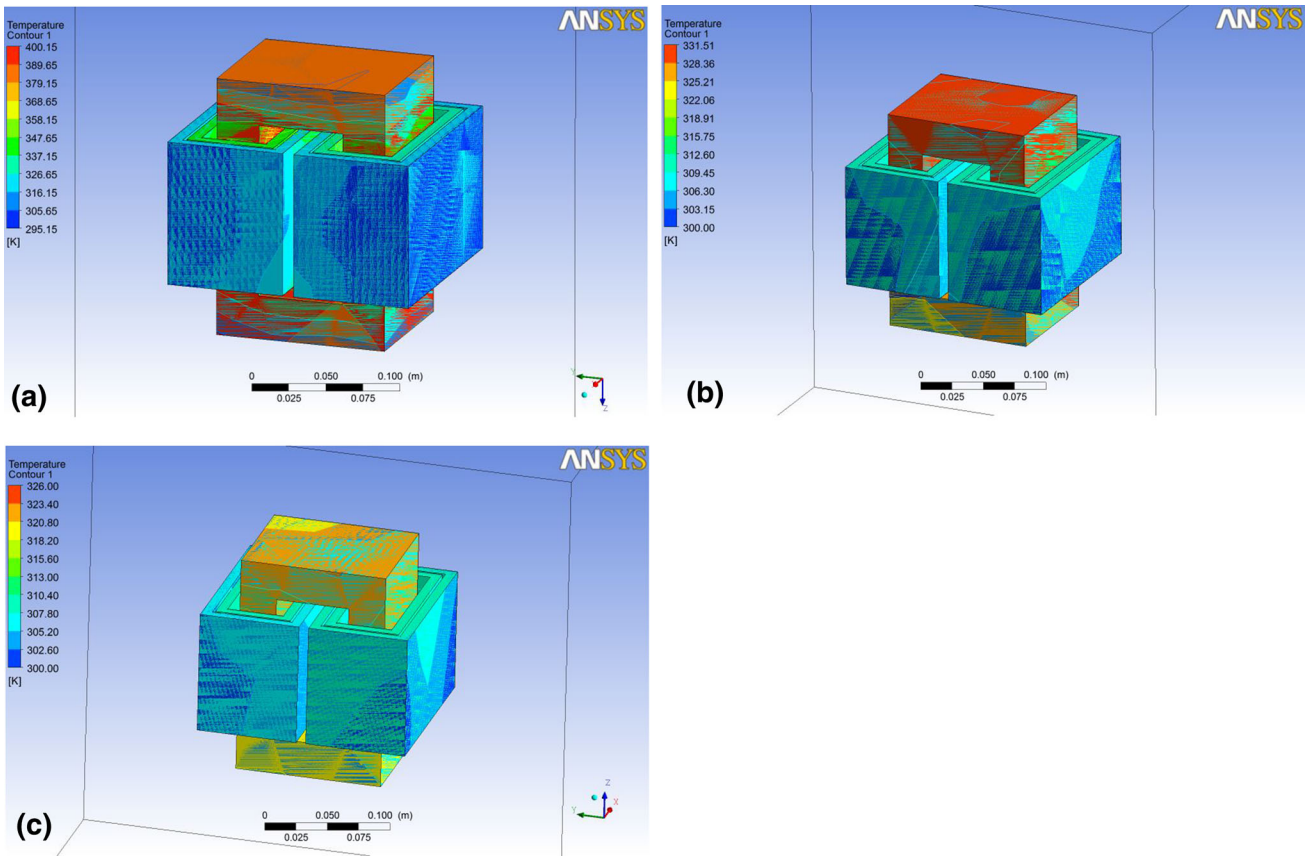

Fig. 6. Heat distribution on the transformer: (a) for maximum 400 K without any air convection, (b) cooling performance with 0.5 m/s air flow velocity for max. 331 K, (c) cooling performance with 1 m/s air flow velocity for max. 331 K.

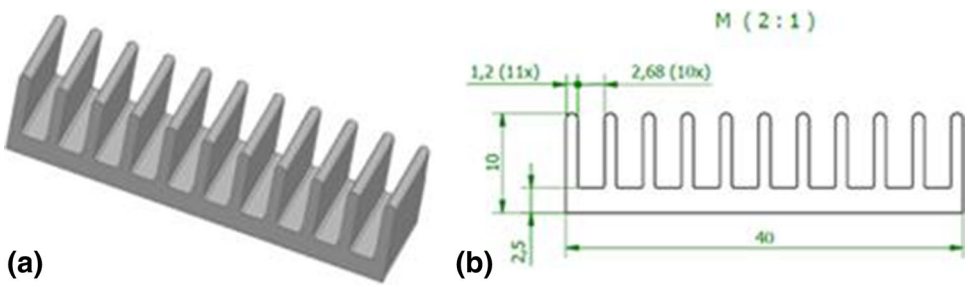

Fig. 7. Aluminum heat sink: (a) 3D FEA model, and (b) sizing the heat sink (sk547).

Thermal Performance of Forced-Air Cooling with Aluminum Heat Sinks

Aluminum heat sinks were mounted at the top and bottom of the core, as shown in Fig. 7, to examine the effects on the thermal performance.[33] Here, the heat in the core is transfered to the external environment with the help of air flow. Therefore, a much more efficient cooling method than forced-air cooling can be realized.

Additional cooling for the windings is not considered because the temperature of the transformer windings is not too high. The temperature distribution for maximum 372 K with a heat sink without any air convection is given in Fig. 8a. Here, approximately 29°C of cooling is realized only with the aluminum heat sink. The air convection is circulated through the x-plane with velocity values of 0.5 m/s and 1 m/s. For this condition, the temperature distributions are given in Fig. 8b and c for max. 324 K and 319 K, respectively.

It is seen that the cooling performance for the transformer core is improved by using the additional heat sinks mounted on the transformer core, and because of this, only air convection cooling in the windings was applied. The cross-sectional area values of the conductors are determined for current density of 2 A/mm^2. Thus, extreme temperature increases in the windings are prevented without any additional cooling. Finally, the temperature distribution is given in Fig. 9 for maximum 317 K with the aluminum heat sinks and air convection cooling conditions with 1.5 m/s air flow velocity. The temperature of the transformer windings is obtained as approximately 56°C. When the air flow is used, the transformer is cooled to 44°C. In addition, the temperature of the transformer core is reduced from 98°C to 40°C with both the aluminum heat sinks and forced-air convection. Thus, the cooling performance of the transformer with ferrite N87 core is improved by the proposed cooling method.

Comparison of Proposed Cooling Methods

The cooling performance for the air-cooled MF transformer depending on the air flow rate is given in Fig. 10. The cooling performance analysis was carried out for maximum 4 m/s air flow in 0.5 m/s interval steps. Both the thermal behavior of the transformer and the performance of the cooling system can be determined from this graph.

It is seen that efficient cooling can be realized for air flow velocity up to 3 m/s. However, the

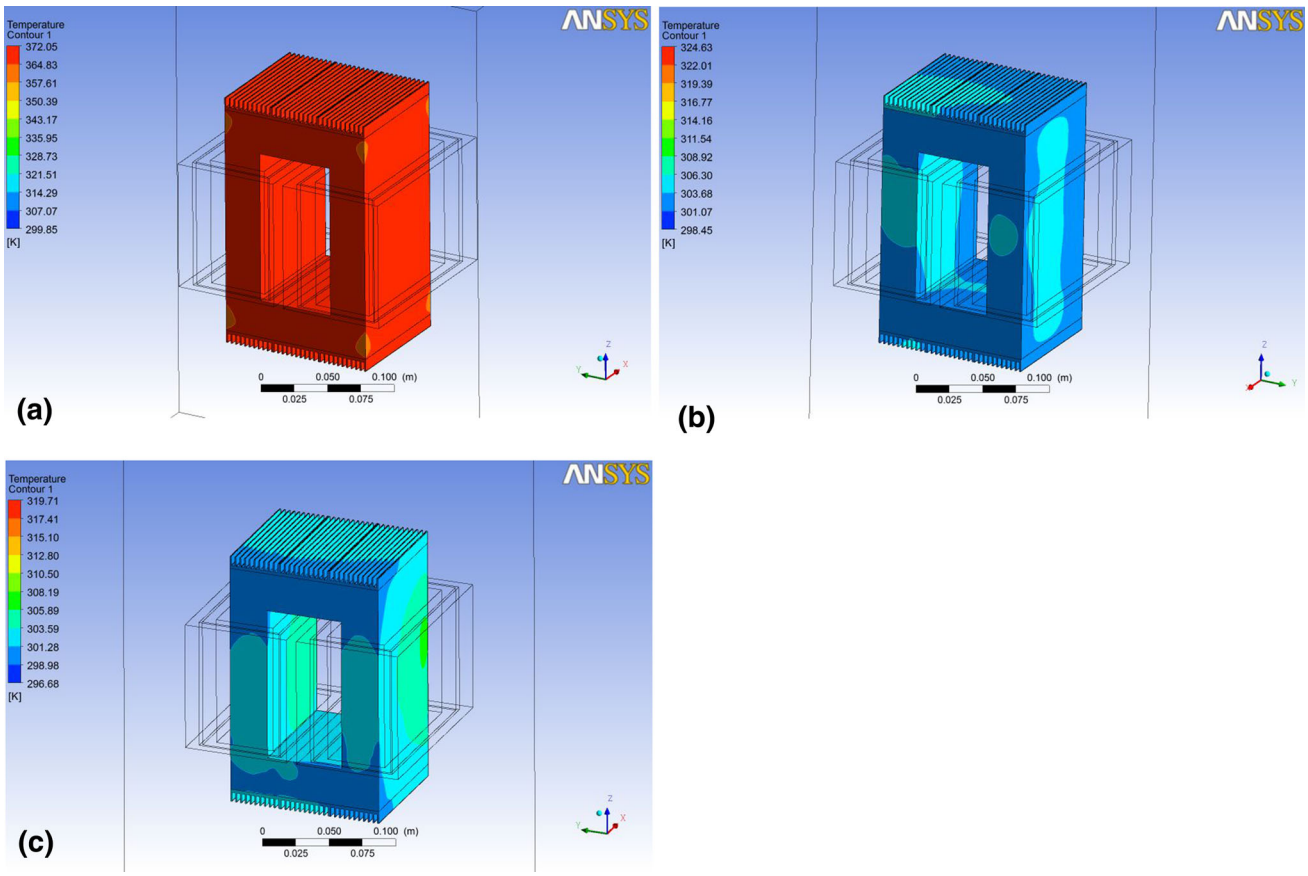

Fig. 8. Cooling performance tests with aluminum heat sinks: (a) without any air convection, (b) with 0.5 m/s fan speed, and (c) with 1 m/s fan speed.

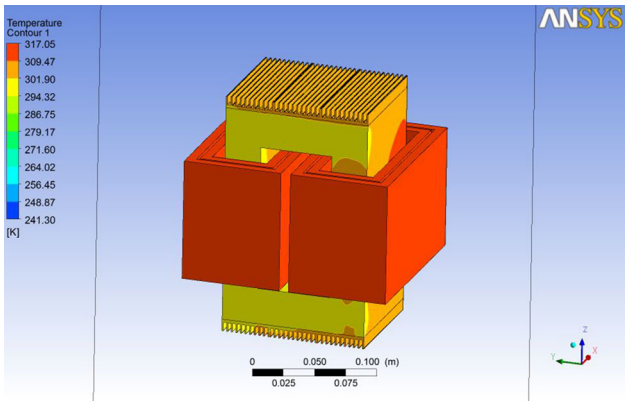

Fig. 9. Temperature distribution on the transformer with aluminum heat sinks.

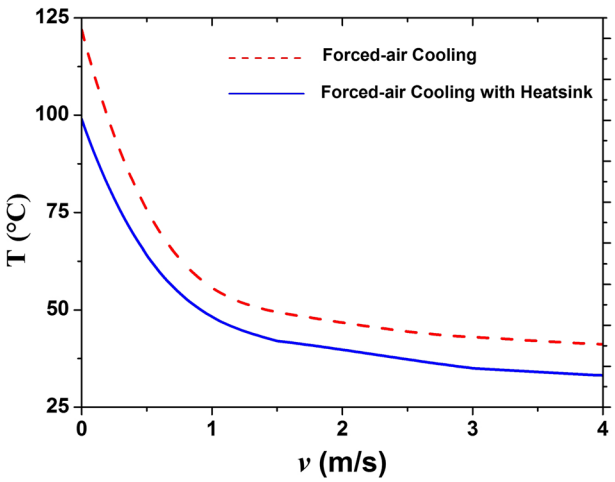

Fig. 10. Cooling capacity depending on air flow velocity.

temperature of the transformer remains constant at 40°C for higher air flow velocity values (≫3 m/s). This means that the cooling performance of a forced-air cooling system remains constant above a certain flow velocity. It is also seen that the level of the cooling capability is better with the aluminum heat sinks. There is a difference of approximately 29°C between the two methods with natural convection. In addition, the cooling performance is improved with forced-air convection, with a difference of 8°C between the two cooling strategies for 3 m/s air flow velocity.

CONCLUSIONS

A 35-kVA MF transformer with ferrite N87 core material was designed and thermally analyzed. In addition, the thermal behavior of the MF transformer with ferrite N87 core was determined for 10 kHz operating frequency and rectangular wave excitation condition. Heat sources of the transformer were investigated, and the temperature of the transformer obtained as 127°C for 22°C ambient temperature without additional cooling. Since this temperature value may become dangerously high for higher ambient temperature, different cooling methods such as forced-air convection, natural convection with additional heat sinks, and additional heat sinks supplied with forced-air convection were analyzed. It is seen that the maximum transformer temperature is obtained as 65°C for forced-air convection with 0.5 m/s air flow velocity. In addition, the transformer temperature is decreased to 98°C with additional heat sinks, and to 40°C for additional heat sinks supplied with forced-air convective cooling. Furthermore, the variation of the cooling system performance with air flow velocity is also analyzed. It is seen that higher air flow velocity values (≫3 m/s) do not provide any additional cooling. On the other hand, mounting additional aluminum heat sinks is proposed to improve the cooling performance. Aluminum heat sinks are mounted to the top and bottom of the transformer core, and the behavior of the MF transformer under nonlinear excitation condition investigated for different cooling conditions. Thus, the thermal behavior of the ferrite N87 core material changed with the aluminum heat sinks, and the cooling performance of the transformer was improved by approximately 29°C for natural convection and 8°C for forced-air convection (with 3 m/s air flow velocity).

REFERENCES

1. I. Sefa, S. Balci, and M.B. Bayram, in *6th Int. Conf. on Electron. Computers and Artificial Intelligence* (*ECAI*): (2014), pp. 43–48.
2. J.M. Silveyra, P. Xu, V. Keylin, V. Degeorge, A. Leary, and M.E. Mchenry, *J. Electron. Mater.* 45, 1 (2015).
3. Villar, L. Mir, I. Etxeberria-Otadui, J. Colmenero, X. Agirre, and T. Nieva, in *IEEE Energy Conversion Congr. and Exposition* (*ECCE*): (2014), pp. 684–690.
4. I. Villar, Dissertation thèse no 4622, EPFL, Lausanne, Switzerland (2010).
5. I. Villar, U. Viscarret, I. Etxeberria-Otadui, and A. Rufer, in *IEEE 34th Annu. Conf. Ind. Electron*. (*IECON*): (2008), pp. 1033–1038.
6. H. Gor and E. Kurt, *Int. J. Hydrog. Energy* (2016). doi: 10.1016/j.ijhydene.2015.12.172.
7. H. Babaie and H. F. Farahani, *J. Electromagnetic Anal. Appl.* 2, 627 (2010).
8. G. Ortiz, J.Biela, and J.W. Kolar, in *IEEE 36th Annu. Conf. on Ind. Electron*. (*IECON*): (2010), pp. 631–638.
9. H. Hoffmann, and B. Piepenbreier, in *14th European Conf. on Power Electron. Appl*. (*EPE*): (2011), pp. 1–8.
10. H. Hoffmann, and B. Piepenbreier, in *1st Int. Electric Drives Production Conf.* (*EDPC*): (2011), pp. 192–197.
11. I. Sefa, N. Altin, S. Ozdemir, and M. Demirtas, in *19th Int. Symp. Power Electron. Elect. Drives, Automation and Motion* (*SPEEDAM*): (2008), pp. 662–666.
12. I. Sefa, N. Altin, S. Ozdemir, O. Kaplan, and I.E.T. Renew, *Power Gen.* 9, 7 (2015).
13. S. Baek, Degree of Doctor of Philosophy, UMI Number: 3710565, Published by ProQuest LLC (2015).
14. M. Kharezy, Master of Science Thesis, Chalmers University of Technology (2014).
15. H.S. Krishnamoorthy, P. N. Enjeti, I.J. Pitel, and J.T. Hawke, in *7th Int. Power Electron. and Motion Control Conf.* (*ECCE*): (2012), pp. 814–819.
16. A. Hilal, M.A. Raulet, C. Martin, and F. Sixdenier, *J. Electron. Mater.* 45, 10 (2015).

17. P.M. Nicolae, D. Constantin, and M.C. Nitu, in *4th Int. Youth Conf. on Energy* (*IYCE*): (2013), pp. 1–5.
18. D. Constantin, P.M. Nicolae, and M.C. Nitu, *IEEE Eurocon*, 1548–1552 (2013).
19. G.Y. Jeong, S.P. Jang, H.Y. Lee, J.C. Lee, S. Choi, and S.H. Lee, *IEEE Trans. Magn.* 49, 5 (2013).
20. Q. Wen, Z. Baohui, H. Zhiguo, and B. Zhiqian, in *Int. Conf. on Power Syst. Techn.* (*POWERCON*): (2014), pp. 826–831.
21. C. Liao, J. Ruan, C. Liu, W. Wen, and Z. Du, *IEEE Trans. Magn.* 50, 11 (2014).
22. M.A. Arjona, C. Hernandez, R. Escarela-Perez, and E. Melgoza, in *Int. Conf. on Electrical Machines* (*ICEM*): (2014), pp. 2270–2274.
23. K. Venkatachalam, C.R. Sullivan, T. Abdallah, and H. Tacca, *IEEE Workshop on Computers in Power Electron.* (2002).
24. I. Villar, A. Rufer, U. Viscarret, F. Zurkinden, and I. Etxeberria-Otadui, in *IEEE Int. Symp. Ind. Electron.* (*ISIE*): (2008), pp. 208–213.
25. P. Dowell, *Proc. in IEEE* 113, 8 (1966).
26. U. Drofenik, in *7th Int. Conf. on Integrated Power Electron. Syst*. (CIPS), (2012).
27. H.J. Lienhard, *A Heat Transfer Textbook* (Cambridge: Phlogiston Press, 2004), pp. 1–6.
28. R. Bargallo, *Finite Elements for Electrical Engineering*, (The Polytechnic University of Catalonia (UPC), Electrical Engineering Department, 2006), http://www.aedie.org/eeej/webrevista/articulos/librosONLINE/EFRBP2006FULL.pdf. Accessed 15 May, 2015.
29. R. Pechanek, and L. Bouzek, in *15th Int. Power Electron. and Motion Control Conf. (EPE/PEMC)*, LS2e.4-1–LS2e.4-5, (2012).
30. W. Xiaowei and L. Tiecai, in *First Int. Conf. on Instrumentation, Measurement, Computer, Communication and Control* (2011), pp. 15–18.
31. R. Wrobel and P.H. Mellor, *IEEE Trans. Magn.* 46, 8 (2010).
32. N. Altin, S. Balci, S. Ozdemir, and I. Sefa, in *IEEE Int. Conf. Renew. Energy Research Appl.* (*ICRERA*): (2013), pp. 1228–1233.
33. Fisher Elektronik GmbH & Co. KG, Aluminum heat sink (sk547). http://www.fischerelektronik.de/web_fischer/en_GB/heatsinks/A01/Standard%20extruded%20heatsinks/VA/SK5471000AL/$productCard/parameters/index.xhtml. Accessed 15 May, 2015.